Clim. Past Discuss., 8, 3613–3655, 2012
www.clim-past-discuss.net/8/3613/2012/
doi:10.5194/cpd-8-3613-2012

Climate of the Past Discussions

Monitoring stable isotopes in caves over altitudinal gradients: fractionation behaviour and inferences for speleothem sensitivity to climate change

V. E. Johnston[1], A. Borsato[1], C. Spötl[2], S. Frisia[3], and R. Miorandi[1]

[1]Geology Section, Museo delle Scienze, Via Calepina 14, 38122 Trento, Italy
[2]Institut für Geologie und Paläontologie, Universität Innsbruck, 6020 Innsbruck, Austria
[3]School of Environmental and Life Sciences, University of Newcastle, Callaghan 2308 NSW, Australia

Received: 30 July 2012 – Accepted: 6 August 2012 – Published: 14 August 2012

Correspondence to: V. E. Johnston (vanessa.johnston@mtsn.tn.it)

Published by Copernicus Publications on behalf of the European Geosciences Union.

Abstract

Large changes of the climate can dramatically affect the environment surrounding and within a cave. This variability, including temperature shifts, can change the amount of in-cave isotopic fractionation affecting speleothems, potentially leaving these records difficult to interpret. Here, caves located in steep altitudinal topography in the Northern Italian Alps are used to create a thermal gradient (3–12 °C) to study the effects of temperature on the speleothem isotope record. The data indicate that the amount of in-cave oxygen isotope fractionation is reduced to minimum values of around 0.25 ‰ with cooler temperatures and under faster dripping stalactites, which infers that such sites would be most suitable for palaeoclimate reconstruction. However, when considering the possible freezing periods, reduced saturation index and fluctuating drip rates, such sites appear less than ideal for study on long timescales. The importance of picking the best site(s) within a cave for palaeoclimate reconstruction is paramount, to reduce the in-cave fractionation and gain a record that reflects climate changes. A method for rapid determination of calcite fractionation is demonstrated here, through prior cave monitoring of dripwaters and calcite precipitates, permitting an informed choice of speleothems for further study.

1 Introduction

Demand for speleothems to be included in palaeoclimate studies is ever increasing due to advances in high-precision dating techniques (Cheng et al., 2009; Wang et al., 2008). Stable oxygen isotopes are most commonly used, being a proxy of environmental changes involving precipitation and temperature (Lachniet, 2009; McDermott, 2004). Application of oxygen isotopes in speleothems has been particularly successful in determining the intensity of the monsoon (Fleitmann et al., 2003; Wang et al., 2001). However, in certain well-constrained cave sites, past temperature reconstructions have also been possible (Boch et al., 2011; Mangini et al., 2005). Nonetheless,

CPD
8, 3613–3655, 2012

the complexity of the oxygen isotope signal is embedded in the fact that the initial rainwater value is controlled by diverse atmospheric processes (e.g. moisture source and transport pathway, altitude and rainfall amount) (Rozanski et al., 1992). This is then modified by evapotranspiration and water-rock interactions as infiltration passes through the soil, host-rock, and into the cave environment as dripwater (Lachniet, 2009; McDermott, 2004). Further alteration then occurs via kinetic fractionation on degassing and the precipitation of speleothem calcite (Day and Henderson, 2011; Mickler et al., 2006; Tremaine et al., 2011). Therefore, robust interpretation of a speleothem archive requires a good understanding of all parts of the oxygen isotope system and the controlling factors for the particular cave and drip site.

Since Genty et al. (2003) found large changes in stable carbon isotopes reflecting Dansgaard–Oeschger Events, reporting of the $\delta^{13}C$ has increased. Carbon isotopes are thought to reflect changes in vegetation and soil above the cave that ultimately reflect temperature-related climate changes. However, the difference between pCO_2 of the dripwater and the cave air, enhanced by cave ventilation, can cause significant enrichment of the $\delta^{13}C$ values (Frisia et al., 2011). Therefore, to fully understand the isotope systematics that affect $\delta^{18}O$ and $\delta^{13}C$, particularly over large-amplitude climate changes, monitoring of the present-day cave environment must take place. Numerous studies are now being carried out to monitor individual caves from which speleothem records are being researched (e.g. Baldini et al., 2006; Mattey et al., 2010; Miorandi et al., 2010; Spötl et al., 2005). However, current conditions are relatively stable when compared to large-amplitude climate events, such as glacial-interglacial boundaries, and therefore monitoring of a single cave will not encompass the entire range of possible hydrological and geochemical conditions that are enclosed in a palaeoclimate archive from that site. Hitherto, there have been little or no studies that attempt to understand how the isotopic system varies under large-amplitude environmental change using cave monitoring field techniques.

Here, changes in altitude, located within a small area of steep topography, are used as a proxy for variations in temperature over time in the palaeoclimate record. A limited

CPD
8, 3613–3655, 2012

amount of monitoring was carried out in eight caves with altitudes between 225 and 1880 m a.s.l. (above sea level) in the Trentino region of North-Eastern Italy (Fig. 1). The monitoring measured changes in the cave air temperatures, cave air CO_2 concentrations, drip rate, basic hydrogeochemistry, and stable isotopes of dripwater and corresponding calcite precipitation and petrography. This is used to assess environmental changes such as the amount of cave ventilation, the state of the soil and vegetation above the cave, and the degree of kinetic fractionation occurring in each cave and at the depositing speleothems. In this study – and probably for the first time ever - data spanning an altitudinal gradient of over 1500 m are brought together for a snapshot in time, to make an assessment of these environmental changes that can affect cave processes and ultimately influence the palaeoclimate record stored in the speleothems in caves at different temperatures. These are interpreted in terms of isotopic processes affecting speleothem records spanning large-amplitude environmental changes, such as glacial-interglacial transitions.

2 Study location

The studied caves are found within dolomite (Late Triassic Dolomia Principale) and limestone (Early Jurassic Calcari Grigi) (Table 1). Vegetation above the caves is controlled by the altitude and also the location of the caves (Fig. 1), whereby the area around Lake Garda receives a more Mediterranean-style climate and other parts of Trentino are temperate-humid to Alpine (high altitude) (Table 1). The present-day timber line lies at 1800 m. The thickness of the rock overburden varies for the cave sites, with some having a shallow overburden (e.g. ER, GZ and CB), whereas others are deeper (e.g. BG, MO and SP). At a number of cave sites, the infiltration water is sourced from an altitude substantially higher than that of the cave entrance due to the steep mountainous topography; hereafter called the "infiltration elevation" (Table 1). In some cases this infiltration elevation could be over 1000 m above the main cave passages (e.g. BG and MO). The caves are mainly hosted within two valleys in Trentino; the main N–S

CPD
8, 3613–3655, 2012

running Adige Valley and a steep E–W running Valsugana Valley. The Adige Valley hosts GZ and CB caves. In addition, DL cave is located in the (N–S) Sarca Valley that heads towards Lake Garda, just off the Adige Valley and MO is situated in a N–S Molveno Lake Valley (parallel to the Adige Valley). The Valsugana Valley contains BG and ER caves with SP located on the Asiago Plateau above (Fig. 1b). FS is the only cave lying at a distance from the other caves to the north of Valsugana Valley.

Mean annual air temperature recorded between 1961 and 1990 in the Adige Valley at Trento (312 m a.s.l.) was 12.3 °C and in Valsugana the temperature at Levico Terme (502 m a.s.l.; Fig. 1) was 11.0 °C. By contrast at high altitudes, the mean annual air temperature was 1.7 °C on Paganella Mountain (2125 m a.s.l) and 7.3 °C at Lavarone (1155 m a.s.l.) on the Asiago Plateau (Fig. 1). Precipitation mean values were 931 mm yr^{-1} at Trento, 1017 mm yr^{-1} at Levico Terme, 729 mm yr^{-1} at Paganella, and 1308 mm yr^{-1} at Lavarone (http://www.meteotrentino.it).

3 Methods

Caves were monitored during September 2010, with the exception of MO (February 2011) and DL that could not be entered until August 2011 due to a flooded entrance (Table 2). In addition, BG was visited on further occasions of August 2010 and February 2012 (Table 2). Carrying out the majority of the monitoring during a single month means that the data represent a snapshot in time, and eliminates much of the temporal variability, seasonal and inter-annual, often exhibited in cave data (e.g. Frisia et al., 2011; Miorandi et al., 2010). During the visits, cave air temperature and cave air pCO_2 concentrations were measured using a Vaisala Meter GM70 with a GMP222 probe (accuracy at 25 °C ± 20 ppm CO_2) at numerous points along the centre of the galleries of each of the caves, to build up a picture of the CO_2 and temperature distribution in addition to the relative strengths of the cave ventilation. Drip rates were timed using a stopwatch, and electrical conductivity, pH and water temperature were measured for the dripwaters and in cave pools. Aliquots were collected from each drip point for

CPD
8, 3613–3655, 2012

isotopic analyses of δ^{18}O and δD. Calcite powders were collected from beneath the corresponding drip points using a Dremel Stylus hand-held, battery operated drill with a diamond wheel point for isotopic analyses (δ^{18}O and δ^{13}C). On selecting drip points, only those with seemingly active (wet and bright) calcite precipitates were chosen, and milling was carried out carefully to remove only surface calcite close to the point of impact.

Isotopic analyses of dripwaters and calcite powders were carried out at the University of Innsbruck, Austria using an on-line, continuous-flow system (Gasbench II) linked to a Thermofisher DELTA^{plus}XL isotope ratio mass spectrometer. The water oxygen isotope composition was determined by equilibration with carbon dioxide and calibrated against VSMOW, GISP and SLAP standards and reported on the VSMOW scale. The 1σ analytical uncertainty on δ^{18}O values is 0.09 ‰ (Spötl et al., 2005). The calcite oxygen and carbon isotopes are reported against VPDB and are calibrated against an in-house standard that has itself been calibrated with NBS-18, NBS-19, CO-1 and CO-8 reference materials. The long-term 1σ standard deviation is 0.06 and 0.08 ‰ for δ^{13}C and δ^{18}O, respectively (Spötl and Vennemann, 2003).

Petrographic analysis was carried out using an optical microscope and a scanning electron microscope (SEM) at the Museo delle Scienze, Trento, Italy. This allowed the observation of calcite material that had been collected under previous long-term monitoring studies, including precipitates on glass plates and stalagmite tops.

4 Results

4.1 Cave air temperature and pCO_2

Figure 2 shows the average air temperature (mean over 1961–1990) from meteorological stations (http://www.meteotrentino.it) with the cave air temperatures measured during monitoring. As expected, the temperature decreases with altitude and in most cases the internal cave air temperatures follows this trend closely. However, one of the

CPD
8, 3613–3655, 2012

monitored caves, BG, has a greatly reduced air temperature for its given cave entrance elevation.

Cave air ventilation may have some effect on the cave temperature, but mostly only close to the entrance. However, ventilation strongly effects cave air pCO_2 concentrations and may subsequently influence kinetic isotope effects. Figure 3 demonstrates the strong increase in cave air pCO_2 with decreasing altitude for most of the cave sites. Again BG cave is an outlier to the general trend, exhibiting lower pCO_2 values than expected for its given altitude. In the highest altitude cave site monitored here, CB cave, most of the passages were at approximately atmospheric CO_2 concentration, with a slight increase in pCO_2 found in a small, secluded chamber, which coincided with the only, possible currently active, speleothem growth in the cave.

4.2 Cave dripwater oxygen and hydrogen isotopes

The oxygen isotope values of the dripwaters collected from caves exhibit decreasing values with increasing altitude (Fig. 4a). The two valleys show distinct isotopic characteristics and therefore must be treated separately when identifying patterns and trends. The Adige Valley generally exhibits lower $\delta^{18}O$ values that range between −11.8 and −8.9‰, and a steeper gradient with altitude ($\Delta\delta^{18}O/100\,m = -0.15$‰). This is in contrast with the Valsugana Valley that generally exhibits a more constant oxygen isotope values, ranging between −10.0 and −8.4‰ with a shallower altitudinal gradient ($\Delta\delta^{18}O/100\,m = -0.08$‰). A similar pattern is shown in the hydrogen isotopes (Fig. 4b). Where the Adige Valley (−79.2 to −60.1‰) displays a steeper gradient ($\Delta\delta D/100\,m = -0.92$‰), and the Valsugana Valley (−66.8 to −54.9‰) exhibits a shallower gradient with altitude ($\Delta\delta D/100\,m = -0.52$‰).

4.3 Petrography of calcite

Petrography of the forming speleothems is important as it can give clues of the saturation state of the dripwater with respect to calcite, in addition to the drip rate

CPD
8, 3613–3655, 2012

and impurities carried in the dripwater, when these cannot be measured in ancient speleothems. Therefore, characterising the conditions at which the fabric changes from one form to another is critical when dealing with a stalagmite record containing different fabrics. In Fig. 5, fabrics from selected caves monitored during this study are shown. At low altitude, precipitates grown in DL cave show flat faces and a large crystal size (50–150 µm) that would result in a columnar fabric. To reach this large crystal size, the glass plate was left in the cave for only 3 months, indicating (for this region) a relatively fast growth rate. The stalagmite Stal-SP1 from SP cave exhibits a columnar fabric (Fig. 5b). Precipitates grown on glass slides at ER cave (Fig. 5c) display irregular faces interrupted by macrosteps and macrokinks, which lead to lateral overgrowths and finally a microcrystalline to dendritic fabric. The shallow ER cave at mid-altitude required the glass slides to be left in-situ for a whole year for enough precipitate to form to allow study. Stalagmite ER77 exhibits a change in fabric from microcrystalline to dendritic (Fig. 5d) that agrees with what would be expected from the precipitates on glass slide (Fig. 5c).

4.4 Oxygen and carbon isotopes of calcite

Oxygen and carbon isotopes measured on presumably active speleothem cave precipitates exhibit values ranging from −8.84 to −6.1 ‰ and −0.5 to −11.3 ‰, respectively (Table 2). Although a large part of the range of isotopic values is caused by the diverse altitudes and cave settings, each cave also exhibits a spread of calcite values that exceed 1 ‰ in oxygen and 5 ‰ in carbon (Fig. 6). This in-cave variability can be largely attributed to fractionation caused by rapid degassing of CO_2 and calcite precipitation (Day and Henderson, 2011; Mickler et al., 2006). Therefore, in the following discussion, the least fractionated example from each cave, that with the lowest isotopic values (circled in Fig. 6), has been chosen to approximate typical cave values before the complications of kinetic fractionation. This allows the clearer identification of patterns occurring with cave altitude, used to represent temperature changes over large amplitude climate variability.

CPD
8, 3613–3655, 2012

5 Discussion

5.1 Cave air temperature

The general trend of air temperature in the stable interior of the caves closely follows that of the mean annual air temperature (Fig. 2). However, for BG cave, and also to a lesser extent MO and FS caves, the cave air temperatures are lower than expected for the given altitudes. This cooling can be explained by rapid infiltration of cold water and meltwater (in spring) that originates from much higher altitudes than the cave entrance and flows through the cave in active streamways, often flooding the main passages completely during these spring meltwater infiltration events. The very large fluxes of cold water entering BG cave causes a major cooling to the cave air temperature. BG cave is similar to that of a cave situated in the deep vadose zone of the conceptual model of temperature distribution of a karst aquifer (Luetscher and Jeannin, 2004). The temperature difference between the cave air and the outside mean annual air is therefore caused by the infiltration elevation being considerably higher than the cave entrance and main passages (as in BG, FS and MO). In such cases, temperature gradients can occur, causing strong ventilation (as felt in BG cave), which can affect many of the hydrological and geochemical properties of interest.

5.2 Cave air pCO_2

Cave air pCO_2 shows a strong trend to higher values at lower altitudes (Fig. 3). This trend is likely due to the greater CO_2 production as a result of higher root respiration and enhanced microbial activity found at low altitude and under thicker soil cover. Importantly, the thick soil cover provides a seal above the epikarst that causes a large proportion of the CO_2 produced to be transferred downwards, towards the cave, rather than released into the atmosphere. In similarity to the cave air temperature (Fig. 2), BG cave does not fit the trend of the other caves, exhibiting a significantly lower pCO_2 than expected for the cave entrance elevation and given the soil thickness and vegetation

CPD
8, 3613–3655, 2012

type on the valley slope (Table 1). This can be attributed to strong cave air ventilation (wind tube), that could easily be felt during the winter months. BG cave ventilation is enhanced by the strong temperature gradient between the cave and the outside atmosphere caused by the cooling from cold, high-elevation infiltration water, in addition to the large amounts of rapidly flowing water that often flood the cave and cause dramatic changes in the air flow. Both MO and FS caves also exhibit slightly lower pCO_2 than expected for their altitudes, which can also be attributed to enhanced ventilation. At higher altitudes, the pCO_2 in the caves trends towards atmospheric values due to reduced vegetation cover and therefore low CO_2 production rates, in addition to a thinning of the soil which becomes patchy, allowing much of the CO_2 produced to be released to the atmosphere.

5.3 Petrography

Petrography is a tool that can give an indication of saturation state and discharge variability of the cave drip that formed the speleothem, along with the degree of isotopic fractionation it was exposed to during formation. The types of fabrics exhibited by speleothems can be simplified into two end-members, columnar and dendritic. The columnar end-member is the more stable form and is generally considered to be produced from a constant drip rate under a moderate and stable saturation state (calcite saturation index < 0.5), with the degree of isotopic fractionation as either very low or extremely invariable. Conversely, dendritic fabric is often found where the drip rate is flashy, the saturation state strongly fluctuates and the degree of isotopic fractionation rapidly changes (Frisia and Borsato, 2010; Frisia et al., 2000). In between these end-members, the range of fabrics include open columnar and microcrystalline (Frisia and Borsato, 2010). To some extent, these fabrics are controlled by the altitude of the caves, since there is a strong correlation between the saturation state of dripwaters and the altitude (Borsato et al., 2007b), and the correlation between saturation state and petrography (Frisia et al., 2000). The saturation state being controlled by the reduction of soil pCO_2 with increasing elevation, due to decreasing temperature and the associated

CPD
8, 3613–3655, 2012

change in vegetation and reduction in soil thickness. However, the correlation of petrography with altitude is not very strong because other factors must also be accounted for, including the cave hydrology (e.g. drip rate), rock overburden, impurities carried in infiltrating water, slope aspect and surface vegetation.

At low altitude, precipitates grown on glass slides in DL cave show columnar fabric with large crystal sizes (50–150 µm), where flat faces characterise the cleavage rhombohedron and ultimately determine the morphology of the crystals (Fig. 5a). The predominance of flat faces is caused by a high saturation index of the dripwaters with respect to calcite (SI_{CC}) (Borsato et al., 2007b), produced by the high pCO_2 in the soil and epikarst, in addition to a low concentration of other ions and impurities (including organic molecules) in the parent water. Furthermore, degassing at the top of the stalagmite is less intense than in other caves, due to the high pCO_2 of the cave air (Fig. 3). This allows the slow, step advance, growth of the crystals, cumulating to form large flat faced crystals. Figure 5b shows a photomicrograph of the top of a stalagmite from SP cave (Stal-SP1 corresponding to drip site SP1) that was active when removed. The fabric of the stalagmite is columnar, exhibiting both compact and microcrystalline subtypes (Frisia and Borsato, 2010). As in the case of DL, the columnar fabric has been formed from slow growth below a drip devoid of other ions or organic molecules that could perturb the system and thus does not exhibit dark laminae characteristic of the transport of impurities (Borsato et al., 2007a; Smith et al., 2009). However, unlike DL, the SI_{CC} at SP is much lower, but importantly at both cave sites the columnar fabric indicates that the SI_{CC} and the drip rates must have remained particularly constant throughout the growth history. It is therefore reasonable to infer that columnar fabric in speleothems, such as SP1, reflects quasi-equilibrium deposition, although modification of the original dissolved inorganic carbon (DIC) $\delta^{13}C$, by degassing at the stalactite tip, cannot be excluded. The presence of columnar fabric at the high altitude of SP cave (1700 m a.s.l.) is relatively uncommon, but in this case is permitted by the thick rock overburden and seepage flow that enhances the calcite supersaturation just above the threshold for columnar fabric, in addition to filtering out impurities in the dripwater and

CPD
8, 3613–3655, 2012

buffering the drip rate. Columnar fabric has been found in other high altitude situations, such as Milchbach cave, but again the water was sourced through a thick overburden and columnar fabric was only formed during periods of stable cave temperatures with minimal air convection and a continuous water supply, interpreted as occurring during entrance sealing during glacial advance (Luetscher et al., 2011).

At mid-altitude, on a NE-facing, forested slope, precipitates grown on a glass slide over a 1-yr period at ER cave under stalactite T5 (Miorandi et al., 2010) show considerable difference to those at DL cave (Fig. 5c). Overall, the crystals are smaller (10–25 µm) compared with DL, and their form deviates from the smooth faced rhombohedron. Stepped and kinked, more unstable faces are predominant. The presence of macrosteps and macrokinks on the irregular faces allows for the nucleation and growth of "lateral overgrowths" (in the sense of Genty and Quinif, 1996); that is, crystals that grow at an angle relative to the larger individual, dictated by crystallographic geometry. This implies that the system may shift, if drip rate is perturbed, toward porous microcrystalline and even dendritic fabric. This is documented in ER76 stalagmite (Scholz et al., 2012) and can be seen clearly on the top of stalagmite ER77 (located close to T5), which exhibits annually laminated microcrystalline columnar fabric (bottom) grading into highly porous dendritic fabric (top; Fig. 5d). The predominance of small crystals with a high density of macrosteps and macrokinks favour the nucleation of lateral overgrowths, that ultimately give rise to the branching crystals of the dendritic fabric. The expectation, based on this fabric type, that the $\delta^{13}C_{calcite}$ is not in equilibrium with the DIC of the dripwater has been confirmed for ER cave, given a fractionation at the stalagmite tips due to degassing and equilibration with cave air of up to −4 ‰ (Frisia et al., 2011).

At the high-altitude CB cave, the low saturation state of the infiltrating water, caused by low pCO_2, means that calcite precipitation is very scanty and slow (Borsato et al., 2000). Therefore, these examples highlight that altitude plays an important role in the petrography, but other factors must also be accounted for. However, at a singular drip site, many of these factors are not changeable over time, such as slope orientation

CPD
8, 3613–3655, 2012

and depth of overburden (except in the case of radical morphological changes such as landslides, glacial scouring or till deposition). Therefore, at a single drip site, a change in petrography will often reflect a change in temperature and climatic conditions (which we here emulate with a change in altitude).

5.4 Oxygen isotope fractionation

Cave analogue laboratory experiments have shown that temperature exerts a more significant influence on speleothem growth mass than drip rate (Day and Henderson, 2011). With elevated temperatures, and also slower drip rates, the same experiments also found that the $\delta^{18}O_{calcite}$ deviates further from values expected, given the parent water isotopic composition and cave temperature, than under cooler and faster dripping conditions (Day and Henderson, 2011). Here, the important influences of temperature and drip rate on $\delta^{18}O_{calcite}$ fractionation are tested in the cave environment, using altitude to adjust the ambient temperature as an analogue for large amplitude climate-driven temperature changes. For each of the calcite samples, the expected $\delta^{18}O_{calcite}$ has been calculated using the equation of Kim and O'Neil (1997) based on the $\delta^{18}O_{drip}$ and the temperature of the dripwater. The fractionation amount has then been computed as the difference between the expected $\delta^{18}O_{calcite}$ and the $\delta^{18}O_{calcite}$ measured on cave precipitates. In all cases, the expected $\delta^{18}O_{calcite}$ calculated from Kim and O'Neil (1997) gave a lower value than the measured value of cave calcites. This indicates that with respect to the laboratory experiments, the cave precipitates were always enriched in oxygen-18, which likely occurred through the process of non-equilibrium isotopic fractionation during degassing and calcite precipitation (Day and Henderson, 2011; Mickler et al., 2004, 2006). To assess the amount of fractionation occurring in the caves studied, Fig. 7a shows a histogram of the distribution of fractionation amount. Although this is only a small study (N = 46) and our results may be artefacts of sampling (where dripwater and calcite do not correspond temporally), Fig. 7a indicates that the most frequent fractionation amount observed in the studied calcite

CPD
8, 3613–3655, 2012

precipitates was between 0.50 and 0.75 ‰ above the theoretical laboratory values of Kim and O'Neil (1997). Moreover, below a fractionation amount of 0.25 ‰, no precipitates were found in the caves during this study. Although with a larger sampling size statistics on the tails of the distribution would be improved, the absence of any sample within this band of minimal fractionation is noteworthy. It likely signifies that within the vadose cave environment it is rarely, or perhaps impossible to reach the conditions of equilibrium found in the laboratory setting (Kim and O'Neil, 1997). This, therefore, infers that all subaerial speleothems are, to some extent, out of isotopic equilibrium.

A strong relationship exists between the fractionation amount and drip rate (Fig. 7b) within individual cave sites, whereby an increase in drip rate causes a decrease in the amount of fractionation (i.e. the value nears the expected laboratory value). A reasonable explanation for this is that with a faster drip rate there is less time for the drip to sit at the stalactite tip, and also on the stalagmite surface, where it could undergo CO_2 degassing that cause the isotopic disequilibrium. In a drier climate, evaporation of the dripwater must also be considered. However, here the relative humidity of the caves was always higher than 90 % and many caves contained standing pools or flowing water, and thus evaporation is not considered to be a substantial contribution in comparison with CO_2 degassing.

The DIC-depletion and increased evaporation with elevated temperatures shown by laboratory experiments (Day and Henderson, 2011) can be tested with the cave data collected here, using altitude as a method of adjusting ambient temperature. Figure 7c shows the amount of fractionation against the altitude of the cave entrance. With the exception of BG and CB caves, there is a trend towards less fractionated $\delta^{18}O_{calcite}$ with higher altitude, and thus lower temperatures. CB cave precipitates do not fit this trend possibly because the calcite was not active at the time of sampling or was extremely slow growing and the sampling removed a layer of calcite that did not correspond to the sampled dripwater. Alternatively, the relatively low drip rate, in addition to the high ventilation known in the cave from the pCO_2 measurements, could have increased the rate of CO_2 degassing above that expected for this altitude. BG cave does not fit the trend of

CPD
8, 3613–3655, 2012

decreasing fractionation amount with altitude because (as noted in Sect. 5.1) BG cave air is cooled by high-elevation infiltrating waters, giving it an apparent air temperature of a cave between 1000 and 1400 m a.s.l. (Fig. 2). Using this air temperature-based elevation, the amount of fractionation in BG cave then becomes aligned with the altitudinal trend of the other caves. Overall, the conclusion that fast dripping sites in cold caves would be the most suitable for carrying out palaeoclimate work, in terms of reducing the amount of in-cave isotopic fractionation, based on laboratory experiments (Day and Henderson, 2011), is supported here with data from cave sites spanning a range of temperatures and drip rates (Fig. 7).

Fractionation amount has been shown as sensitive to changes in temperature and drip rate (Mühlinghaus et al., 2009). Within a single cave site or cave chamber, factors such as temperature and ventilation are essentially constant. Therefore, in a single cave chamber the variability in the fractionation can be assumed to be due to drip rate and possibly also drip height. In this study, there is only a weak relationship between fractionation amount and drip height. Therefore, the drip rate is considered the primary controlling factor for same-cave (same-chamber) fractionation effects (although drip height requires more detailed investigation). At individual cave sites, the oxygen isotope fractionation amount is shown to be up to approximately 1.5 ‰ (between the least and most fractionated examples), which can be attributed primarily to variations in drip rate that can span three orders of magnitude in a single cave site (Fig. 7b). However, over the range of altitudes and corresponding temperatures (3–12 °C) in this study, the least fractionated examples from each cave, which can be taken as those affected just by the cave temperature and only minimally by drip rate fractionation, range in values by only 1 ‰ (Fig. 7c). A large-amplitude climate change would likely be affected by both a change in temperature and water availability. However, the sensitivity to fractionation of a couple of degrees temperature change (about 0.5 ‰) is much less than the fractionation caused by the dramatic, accompanying change in the drip rate (around 1 ‰ for a two order of magnitude drip rate change).

CPD
8, 3613–3655, 2012

Calcite fractionation is often expressed as the term $1000 \ln \alpha$, with field measurements given as the difference between $\delta^{18}O_{calcite}$ and $\delta^{18}O_{drip}$. Many different estimations of this value over ranging temperature exist from laboratory and theoretical work, based on different conditions or assumptions (e.g. Chacko and Deines, 2008; Coplen, 2007; Friedman and O'Neil, 1977; Kim and O'Neil, 1997; Tremaine et al., 2011). Figure 7d shows that the theoretical values of Chacko and Deines (2008) are lower than the experimentally derived values of Kim and O'Neil (1997). The measurements made in the caves are still higher, with the more fractionated examples exhibiting a greater deviation (higher $1000 \ln \alpha$ values) from the theoretical and experimental values. The red line in Fig. 7d shows an empirical palaeotemperature curve (Tremaine et al., 2011), calculated from speleothems in the literature to demonstrate typical cave water-calcite oxygen isotope fractionation. Calcite precipitates from this study widely range around this empirical speleothem line, given the variety of fractionation amount experienced by the different samples. However, the least fractionated samples plot below the literature line, closer to the experimental values. This indicates that, on average, the speleothems from the literature used to calculate the empirical line were slightly more fractionated than the least fractionated samples found in this study. Therefore, it is possible that more could be done in terms of prior monitoring, in order to select the least fractionated samples from a cave for further study.

The approach taken in this study, to mill a small amount of calcite powder from the tops of calcite speleothems and collect corresponding dripwaters, is a very simple test for isotopic fractionation in a cave. It is only minimally destructive (better still is to collect precipitates on glass slides, if precipitation rates are high and time permits) and can be used as a preliminary test to help choose which speleothems should be removed for further study. The importance of choosing a good speleothem for palaeoclimate reconstruction is critical, since below 10 °C (this study) at a good site the speleothem should exhibit between 0.25–0.5 ‰ fractionation in oxygen, which is less than expected for the large-amplitude climate changes of interest (> 1 ‰). However, at a poorly chosen site, the fractionation could be as large as 1.5–2 ‰, which would completely mask any

CPD
8, 3613–3655, 2012

low-amplitude variability and may be of a similar extent to that of the large-amplitude climate events, meaning that the significance of the oxygen isotope results would be unreliable.

5.5 Oxygen isotopes variability with altitude

Oxygen and hydrogen isotopes of cave dripwater decrease with altitude, but with a steeper gradient in the Adige Valley (Fig. 4). A similar pattern is seen in the annual weighted-mean rainfall (Fig. 8) but with an offset to more enriched values (discussed below). In the more typical situation of the Adige Valley, the wider N–S orientated valley allows the easy passage of moisture to flow down and within the mountains permitting the typical altitudinal rainout pattern expected (Longinelli and Selmo, 2003). However, the Valsugana is a narrow valley, oriented E–W and bounded by high mountains (between 2300 and 1900 m a.s.l.). Air masses, originating from the Mediterranean Sea, travel northwards across the Po Plain before reaching the mountain barrier. Here, the air is forced upwards, and rain-out occurs steadily enriching the moisture carrying air parcel through Rayleigh fractionation. As the moisture reaches the long (E–W) crest of the Valsugana Valley bounding mountains, the rain that falls at both high and low altitudes in the valley exhibits very similar isotopic compositions as there is not much differentiation in source between elevations.

In the Valsugana Valley (Fig. 8a), dripwater $\delta^{18}O$ is slightly depleted with respect to that of the annual weighted-average rainwater value (Bertò et al., 2005). This is because infiltration occurs mainly during autumn and spring (winter snowmelt) due to evapotranspiration in summer. During these infiltration seasons, the $\delta^{18}O$ value is lower than in summer, resulting in lower $\delta^{18}O_{drip}$ than the annual weighted-average rainwater value. This can be termed the weighting effect and should be quantifiable through the Thornthwaite method (Thornthwaite, 1948), accounting for strong evapotranspiration in the summer months. This weighting effect has also been shown to be important in oxygen isotope enabled rainwater to cave dripwater and stalagmite models (Wackerbarth et al., 2012), and therefore quantifying its value with real data

CPD
8, 3613–3655, 2012

over varying altitudes, latitudes and slope aspects is critical for testing the reliability of such models. For Valsugana Valley caves, their northerly aspect keeps low altitudes shaded, while the high plateau is a well-vegetated, sunny meadow, causing a relatively constant evapotranspiration rate, and thus weighting effect, over the entire altitudinal gradient. The overall slope of the rainwater ($\Delta\delta^{18}O/100\,m = -0.08\,‰$) and dripwater $\delta^{18}O$ (offset by a constant weighting effect) curves is rather shallow, caused by the E–W orientation of the Valsugana Valley. Given this shallow slope and the influence of the decreasing temperature with altitude, the theoretical $\delta^{18}O$ value for calcite (Kim and O'Neil, 1997) anywhere in the Valsugana Valley, independent of altitude, has been calculated as $-7.7 \pm 0.2\,‰$ (Fig. 8a). This means that due to the geomorphological setting and rainfall trajectories predominantly from the Mediterranean, caves of the Valsugana Valley would not be suitable for the reconstruction of palaeo-temperature changes using oxygen isotopes. $\delta^{18}O$ measured on calcite precipitates in the Valsugana Valley caves, however, exhibit a slightly negative trend with altitude. This is caused by the amount of isotopic fractionation that, as shown in Sect. 5.4, decreases with altitude and thus reduces with a lowering of the cave temperature. The affect of this reduction in fractionation at higher altitudes causes the measured calcite to resemble the original source water.

In the Adige Valley (Fig. 8b), the situation is different due to its N–S orientation. The meteoric $\delta^{18}O$ trend follows a steeper ($\Delta\delta^{18}O/100\,m = -0.22\,‰$) and more typical slope, with altitude. The cave dripwater again exhibits lower values due to autumn and (winter) spring infiltration via the weighting effect. However, the cave dripwater does not run parallel to the rainwater but tends towards the rainwater slope at high altitude. This is caused by higher evapotranspiration occurring at low altitudes, particularly in the Mediterranean climate around DL cave, and by reduced evapotranspiration at high altitudes where vegetation is sparse. Seasonal weighting of oxygen isotopes therefore changes with altitude, between a strong winter signal in hot, low altitude climates to almost no weighting at cold, high altitude cave sites. At the warm, low altitude cave site (DL), the difference between the rainfall and cave dripwater measured here was

CPD
8, 3613–3655, 2012

around 1 ‰. Therefore, this effect needs to be more carefully accounted for in cave monitoring studies so that it can be effectively included and tested for in oxygen isotope enabled, rainwater-forced, dripwater-stalagmite models (e.g. Wackerbarth et al., 2012), particularly where cave sites of varying altitudes and latitudes are modelled.

The calculated $\delta^{18}O_{calcite}$ of the Adige Valley exhibits a curved trend due to the strong influence of temperature on the water isotopes and the cave air. The measured cave $\delta^{18}O_{calcite}$ exhibits a similar trend to that calculated but with a deviation to slightly higher values at low altitudes due to the greater fractionation (Fig. 7). Overall, the change in oxygen isotopes measured in cave calcite over the altitude range of the Adige Valley exceeds the minimal changes in isotopic fractionation. Therefore, at well-chosen drip sites, changes in temperature associated with climate variability should be recognisable, and possibly quantifiable, in the $\delta^{18}O$ speleothem record.

However, one outlier CB cave $\delta^{18}O_{calcite}$ has a higher value than expected for its altitude. This is possibly due to strong fractionation of this sample and, as discussed in Sect. 5.4, may be caused by the calcite not being active or being extremely slow growing. Moreover, the slow growing nature of the CB calcite (and also calcite at certain drip points in other caves) may have meant sampling removed a considerable number of years of growth from the top of the speleothems. Long-term monitoring in the region has shown that substantial seasonal and inter-annual variability in $\delta^{18}O$ can be seen in the rainwater and cave dripwater, caused by differing trajectories and climate settings, such as North Atlantic Oscillation (Scholz et al., 2012). For example, monitoring of GZ cave has shown a period where $\delta^{18}O_{drip}$ were considerably higher during the years 2002 (-9.2 ± 0.2 ‰) and 2003 (-9.2 ± 0.2 ‰) owing to a lack of winter snowfall (Frisia et al., 2007), compared with measurements taken during this study (-10.3 ± 0.1 ‰, Table 2). In GZ cave, growth rates on the candlestick shaped stalagmites are high, at approximately 260 µm yr^{-1} (Frisia et al., 2007), and therefore only the recent growth is likely to have been sampled. However, other sites in Trentino would have been subjected to the same inter-annual variability, and under a slow growth rate, could exhibit substantially higher $\delta^{18}O_{calcite}$ compared to the present-day dripwater due

CPD
8, 3613–3655, 2012

to this period of enriched source water. Although the method presented here is quick to gain results, and can thus be used to rapidly identify speleothems for further study, caution is required when comparing the speleothem calcite with the dripwater, as there is no assurance that they are comparable. For an improved accuracy, precipitates grown on glass slides are recommended. However, in slow growing sites such as the cool Alpine caves studied here, as much as a year or mores growth may be needed to acquire enough material to make one isotopic analysis, which is not suitable for a rapid reconnaissance study.

5.6 Carbon isotopes of speleothem calcite

Cave calcite carbon isotope values exhibit a strong increasing pattern with altitude (Fig. 9a). The reason for this is likely that at low altitude, the rich vegetation and thick soil coverage gives a strongly negative, biogenic $\delta^{13}C$ signal. Whereas at high altitude, the cooler conditions permit only sparse vegetation and a thin, patchy soil cover causing a $\delta^{13}C$ signal that is much closer to that of the atmosphere with a small contribution from the bedrock. As previously discussed (Sect. 5.2), the thicker soil at low altitudes acts as a trap, forcing a larger amounts of CO_2 downwards into the epikarst and aquifer, rather than being released into the atmosphere, enhancing the cave air pCO_2 at low altitudes (Fig. 3). In Fig. 9b, the caves with higher cave air pCO_2 also exhibits calcite precipitates with lighter ^{13}C values, indicating a predominance of biogenic sourced carbon from the soil. Whereas at low altitudes, the calcite $\delta^{13}C$ signal is a combination of atmospheric, soil-biogenic and bedrock carbon that has been modified by in-cave fractionation processes (Frisia et al., 2011).

Theoretical experiments have shown that in-cave isotopic fractionation caused by elevated temperatures and higher dripwater pCO_2 would result in higher $\delta^{13}C$ values of the precipitated calcite (Mühlinghaus et al., 2009). However, such a relationship would cause the altitudinal (temperature) trend shown in Fig. 9 to shift to a more vertical slope. Therefore, it is possible to infer that in comparison to the strong signal acquired from the vegetation and soil, $\delta^{13}C$ fractionation due to temperature and pCO_2 are minimal.

CPD
8, 3613–3655, 2012

Conversely, forced degassing of dripwater due to cave ventilation has been shown to cause enhanced kinetic C-isotope fractionation, resulting in ^{13}C enrichment in calcite precipitates (Frisia et al., 2011; Spötl et al., 2005). Ventilation is especially strong in CB cave, which hosts many entrances at different altitudes and a strong seasonal variability in temperature, in addition to those caves with active running water, including DL, BG, MO, FS and SP. Therefore, C-isotope fractionation is likely caused by forced degassing and is thus expected to exhibit some seasonal variability and correlation with drip rate (Frisia et al., 2011; Spötl et al., 2005). It is possible that this type of forced degassing fractionation is stronger at higher elevations, due to the stronger seasonal variability in temperatures and saturation state of drip water. Such an increase in fractionation at high elevation would enhance the relationship in Fig. 9a, seemingly causing a stronger connection between $\delta^{13}C$ and altitude (temperature).

Calcite from Bigonda cave (BG) consistently shows higher $\delta^{13}C$ values than expected given its altitude (Fig. 9a). This is due to the water feeding the BG drips being sourced from a much higher altitude than the cave entrance, also seen in Figs. 2 and 3 of cave temperature and pCO_2. The $\delta^{13}C$ signal is picked up from where the water infiltrates the bedrock, which according to Fig. 9a is around 1000 m a.s.l However, the temperature of the cave water indicates that the infiltration water derives from approximately 1700 m a.s.l. (Fig. 2), while cave air pCO_2 is low due to strong ventilation (Fig. 3). The oxygen isotopes cannot be used to resolve this discrepancy because of the setting in the Valsugana Valley causing little $\delta^{18}O$ change with altitude (Sect. 5.5). Therefore, it is suggested that the dripwater for this part of the cave only is sourced from around 1000 m a.s.l., on the mountain slope, based on the $\delta^{13}C$ vegetation signal. However, the cave also receives a large amount of infiltration from higher altitude that acts as a cooling system to the extensive network of passages. The $\delta^{13}C$ values therefore indicate a maximum of 1000 m a.s.l. for the sampled drips in BG cave, since they likely also suffer from forced degassing caused by the large influx of flowing water, wide seasonal temperature variations and strong ventilation.

CPD
8, 3613–3655, 2012

5.7 Implications for speleothem-based palaeoclimate studies

In this study, caves distributed along a steep altitudinal gradient have been used to mimic the temperature change observed over large-amplitude climate events. Fractionation of the oxygen isotope signal can be a large problem (Mickler et al., 2006). Even in the least fractionated speleothem samples, the smallest amount of oxygen isotope fractionation is on the order of 0.25 ‰ (Fig. 7), compared with laboratory measurements (Kim and O'Neil, 1997). This isotopic fractionation can obscure a temperature signal or information on the original composition of the dripwater. However, when interpreted correctly it could provide alternative climatic information such as amount of ventilation affecting the cave. In agreement with laboratory studies (Day and Henderson, 2011), the data presented here supports the relationship showing a decrease in the amount of oxygen isotope fractionation with a reduction in temperature or an increase in the drip rate. Therefore, in general, cool and fast dripping cave sites lacking strong ventilation should be most suitable for palaeoclimate reconstructions, as they will be least affected by kinetic fractionation.

Of interest here, however, is what will happen in terms of isotopic fractionation and petrography over a large-amplitude climate change that would affect cave air temperature, pCO_2 and outside soil and vegetation. For oxygen isotopes, the predominant driving force causing the climate-related isotopic shift must be considered. As an example of two end-member environmental situations, we extrapolate our findings to consider caves where the oxygen isotope composition is dominated by rainfall changes through the amount effect, such as those in monsoon regions (e.g. Wang et al., 2001), and alternatively caves where $\delta^{18}O$ is controlled by temperature changes. During a warm and humid climate period, such as an interstadial, a rainfall (amount effect)-dominated cave would record a relatively low $\delta^{18}O$ signal (compared with a cool and dry period), which is then modified by in-cave fractionation. In this case, there should be minimal fractionation as the wet environment would allow a high drip rate. Moreover, with a high calcite saturation index and steady drip rate the fabric is likely to be an equilibrium form

CPD
8, 3613–3655, 2012

such as columnar. If the cave temperature was high, the fractionation amount may be higher. However, in the case of many Asian monsoon caves, the cave air temperature is relatively low, 8–9 °C at Sanbao Cave (Cheng et al., 2009) and 15.4 °C at Hulu Cave (Wang et al., 2001). Therefore, a low to average fractionation amount can be expected during warm periods causing only slight enrichment of the oxygen isotope signal. Conversely, under a cooler and drier climate, a rainfall-dominated cave would exhibit a high $\delta^{18}O$ signal that would be affected by fractionation, due to drying of the drip sites and a lowering of the drip rate, causing $\delta^{18}O$ enrichment to even heavier values. Although the temperature would cool, it is unlikely to cool to an extent large enough to significantly lower the fractionation amount (steep part of Fig. 7c). The high $\delta^{18}O$ would likely be accompanied by a change in fabric to a disequilibrium form, such as dendritic, due to cooler temperatures and therefore a lower SI_{CC} and possibly a flashy drip rate, that could augment the fractionation further. Overall, in a rainfall-dominated speleothem record, the in-cave oxygen isotope fractionation shifts the signal in the same direction as the climate-related change, thus amplifying the apparent climate signal.

This is in contrast to caves where the oxygen isotope records are dominated by temperature. Warm climates tend to cause high $\delta^{18}O$ values in meteoric precipitation and hence in the dripwater (Fig. 8; in comparison with cool climates). A speleothem record would then be modified by an average amount of in-cave fractionation based on warm but relatively wet conditions with a columnar fabric. The overall shift under the warm climate in a temperature-dominated environment is to slightly higher $\delta^{18}O$ values. Under cool and dry climates, the temperature-dominated speleothem records low $\delta^{18}O$ values (in comparison with warmer climates). These are then modified by an average to high amount of fractionation on account of the water stress. The cool and dry climate will cause a lower and fluctuating drip rate, eventually enriching the calcite $\delta^{18}O$ values, but also leading to a microcrystalline or dendritic fabric that may cause further fractionation to the calcite $\delta^{18}O$ values. Overall, in the temperature-dominated cave setting, fractionation does not strengthen the climate signal, often working in the

CPD
8, 3613–3655, 2012

opposite direction, and therefore, strong changes in fractionation could mask climate and environmental signals from oxygen isotopes.

Carbon isotopes in speleothem calcite are dominated by the vegetation signal and relationship with soil pCO_2 (Fig. 9). Under warm humid climates, such as interstadials, the $\delta^{13}C$ values will be low due to a greater biogenic contribution. Moreover, there will be relatively little fractionation due to fast drip rates and therefore a shorter time for degassing at the stalactite tip. By contrast, during cool and dry climate periods, such as stadials, the $\delta^{13}C$ values will increase due to reduced vegetation and microbial activity in the soil, and therefore a lower biogenic contribution. Drying will cause a reduction in the drip rate that will enhance forced degassing and thus cause a higher amount of fractionation, increasing the $\delta^{13}C$ values further. Therefore, fractionation of $\delta^{13}C$ values works in the same direction as the climate change, to apparently amplify the signal. This is possibly the reason why the carbon isotope signature can, in some cases, be more successfully interpreted than the oxygen isotope signal (e.g. Genty et al., 2006; Hodge et al., 2008; Scholz et al., 2012), especially where the latter is dominated by temperature. Nonetheless, the carbon isotope signature can be complicated by the different proportions of $C_3 : C_4$ plants in certain regions of the world and under particular climate conditions. Furthermore, the fractionation on carbon isotopes is enhanced by forced degassing, which is greater under conditions of high seasonality. Certain periods of Earth history, such as those with high obliquity, for example during the Eemian (e.g. Felis et al., 2004), are thought to exhibit high seasonal contrast. Therefore, such periods may produce higher $\delta^{13}C$ values than expected, given the vegetation and soil coverage, due to enhanced seasonal temperature changes causing increased ventilation and thus greater degassing and more fractionation.

6 Conclusions

A steep altitudinal topography has been successfully employed to investigate the role of vegetation, soil and temperature changes on cave characteristics and speleothem

CPD
8, 3613–3655, 2012

calcite isotopic composition. In agreement with laboratory experiments (Day and Henderson, 2011), oxygen isotope fractionation was found to decrease in cooler caves under faster dripping stalactites. However, under the very cool temperature conditions required for minimal oxygen isotope fractionation (≤ 0.25 ‰), a large-amplitude climate change could risk imposing periods of water stress, due to ice and snow build-up, or undersaturation with respect to calcite. Such conditions would impose drip rate fluctuations causing greater isotopic fractionation or periods of non-deposition (hiatuses). Whereas, in a warmer temperate environment, although the oxygen isotope fractionation due to temperature will be slightly larger, the possible variability of drip rate is lower, resulting in lower overall fractionation amounts spanning large-amplitude climate changes and little risk of hiatuses. Furthermore, in rainfall-dominated environments, such as monsoon areas, in-cave fractionation tends to work in the same direction as the climate influence, strengthening the apparent signal. However, in temperature-dominated environments, the oxygen isotope record is likely complicated by in-cave fractionation that shifts in the opposite direction to the climate influence. In-cave fractionation of the carbon isotope tends to shift in the same direction as the climate change, and therefore in certain cases where there are no further complications from varying $C_3 : C_4$ proportions, the $\delta^{13}C$ record may provide an alternative climate proxy. Since many factors contribute to the amount of fractionation affecting calcite isotope composition and the speleothem fabric, individual caves and drip sites must be studied in detail to gain an understanding of these controlling influences. Although much can be learned from theoretical modelling and controlled laboratory experiments, they are no substitute for monitoring in the real cave environment.

Acknowledgements. This work have been carried out within the INTCLIM project co-funded by the European Commission under the 7th Framework Programme Marie Curie Actions Scheme and the Autonomous Province of Trento (PAT). For cave access, we would like to thank the Gruppo Grotte Selva di Grigno (BG Cave) and Gruppo Grotte Trevisol-CAI Vicenza (SP Cave). We appreciate the laboratory help of M. Wimmer (Innsbruck) and N. Angeli (SEM, Trento) and field support of M. Zandonati (Trento).

CPD
8, 3613–3655, 2012

References

Baldini, J. U. L., McDermott, F., and Fairchild, I. J.: Spatial variability in cave drip water hydrochemistry: implications for stalagmite paleoclimate records, Chem. Geol., 235, 390–404, 2006.

Bertò, A., Borsato, A., Frisia, S., Miorandi, R., and Zardi, D.: Monthly isotopic signal of the precipitated water in the Province of Trento: Lagrangian analysis and discussion of measurements, in 28th International Conference on Alpine Meteorology, Vol. 40, 432–435, Croatian Meteorological Journal, Zadar, Croatia, 2005.

Boch, R., Cheng, H., Spötl, C., Edwards, R. L., Wang, X., and Häuselmann, Ph.: NALPS: a precisely dated European climate record 120–60 ka, Clim. Past, 7, 1247–1259, doi:10.5194/cp-7-1247-2011, 2011.

Borsato, A., Frisia, S., Jones, B., and Van der Borg, K.: Calcite moonmilk: crystal morphology and environment of formation in caves in the Italian Alps, J. Sediment. Res., 70, 1171–1182, 2000.

Borsato, A., Frisia, S., Fairchild, I. J., Somogyi, A., and Susini, J.: Trace element distribution in annual stalagmite laminae mapped by micrometer-resolution X-ray fluorescence: implications for incorporation of environmentally significant species, Geochim. Cosmochim. Ac., 71, 1494–1512, 2007a.

Borsato, A., Miorandi, R., Corradini, F., and Frisia, S.: Idrochimica delle acque ipogee in Trentino: specie, variabilità stagione, gradiente altitudinale e implicazioni per gli studi climatico-ambientali da speleotemi, Studi Trentini di Scienze Naturali, Acta Geologica, 82, 123–150, 2007b.

Chacko, T. and Deines, P.: Theoretical calculation of oxygen isotope fractionation factors in carbonate systems, Geochim. Cosmochim. Ac., 72, 3642–3660, 2008.

Cheng, H., Edwards, R. L., Broecker, W. S., Denton, G. H., Kong, X. G., Wang, Y. J., Zhang, R., and Wang, X. F.: Ice age terminations, Science, 326, 248–252, 2009.

Coplen, T. B.: Calibration of the calcite-water oxygen-isotope geothermometer at Devils Hole, Nevada, a natural laboratory, Geochim. Cosmochim. Ac., 71, 3948–3957, 2007.

Day, C. C. and Henderson, G. M.: Oxygen isotopes in calcite grown under cave-analogue conditions, Geochim. Cosmochim. Ac., 75, 3956–3972, 2011.

CPD
8, 3613–3655, 2012

Felis, T., Lohmann, G., Kuhnert, H., Lorenz, S. J., Scholz, D., Patzold, J., Al-Rousan, S. A., and Al-Moghrabi, S. M.: Increased seasonality in Middle East temperatures during the last interglacial period, Nature, 429, 164–168, 2004.

Fleitmann, D., Burns, S. J., Mudelsee, M., Neff, U., Kramers, J., Mangini, A., and Matter, A.: Holocene forcing of the Indian monsoon recorded in a stalagmite from Southern Oman, Science, 300, 1737–1739, 2003.

Friedman, I. and O'Neil, J. R.: Compilation of stable isotope fractionation factors of geochemical interest, in: Data of Geochemistry, 6th Edn., US Geol. Surv. Prof. Paper 440-KK, KK1–KK12, Washington, USA, 1977.

Frisia, S. and Borsato, A.: Karst, in: Developments in Sedimentology, Carbonates in Continental Settings, edited by: Alonso-Zarza, A. M. and Tanner, L. H., Elsevier, The Netherlands, 269–318, 2010.

Frisia, S., Borsato, A., Fairchild, I. J., and McDermott, F.: Calcite fabrics, growth mechanisms, and environments of formation in speleothems from the Italian Alps and Southwestern Ireland, J. Sediment. Res., 70, 1183–1196, 2000.

Frisia, S., Borsato, A., Richards, D. A., Miorandi, R., and Davanzo, S.: Variazioni climatiche ed eventi sismici negli ultimi 4500 anni nel Trentino meridionale da una stalagmite della Cogola Grade di Giazzera, Studi Trentini di Scienze Naturali, Acta Geologica, 82, 205–223, 2007.

Frisia, S., Fairchild, I. J., Fohlmeister, J., Miorandi, R., Spötl, C., and Borsato, A.: Carbon mass-balance modelling and carbon isotope exchange processes in dynamic caves, Geochim. Cosmochim. Ac., 75, 380–400, 2011.

Genty, D. and Quinif, Y.: Annually laminated sequences in the internal structure of some Belgian stalagmites – importance for paleoclimatology, J. Sediment. Res., 66, 275–288, 1996.

Genty, D., Blamart, D., Ouahdi, R., Gilmour, M., Baker, A., Jouzel, J., and Van-Exter, S.: Precise dating of Dansgaard-Oeschger climate oscillations in Western Europe from stalagmite data, Nature, 421, 833–837, 2003.

Genty, D., Blamart, D., Ghaleb, B., Plagnes, V., Causse, C., Bakalowicz, M., Zouari, K., Chkir, N., Hellstrom, J., Wainer, K., and Bourges, F.: Timing and dynamics of the last deglaciation from European and North African delta C-13 stalagmite profiles – comparison with Chinese and South Hemisphere stalagmites, Quaternary Sci. Rev., 25, 2118–2142, 2006.

CPD
8, 3613–3655, 2012

Hodge, E. J., Richards, D. A., Smart, P. L., Andreo, B., Hoffmann, D. L., Mattey, D. P., and González-Ramón, A.: Effective precipitation in Southern Spain (~ 266 to 46 ka) based on a speleothem stable carbon isotope record, Quaternary Res., 69, 447–457, 2008.
Kim, S.-T. and O'Neil, J. R.: Equilibrium and nonequilibrium oxygen isotope effects in synthetic carbonates, Geochim. Cosmochim. Ac., 61, 3461–3475, 1997.
Lachniet, M. S.: Climatic and environmental controls on speleothem oxygen-isotope values, Quaternary Sci. Rev., 28, 412–432, 2009.
Longinelli, A. and Selmo, E.: Isotopic composition of precipitation in Italy: a first overall map, J. Hydrol., 270, 75–88, 2003.
Luetscher, M. and Jeannin, P.-Y.: Temperature distribution in karst systems: the role of air and water fluxes., Terra Nova, 16, 344–350, 2004.
Luetscher, M., Hoffmann, D. L., Frisia, S., and Spötl, C.: Holocene glacier history from alpine speleothems, Milchbach cave, Switzerland, Earth Planet. Sci. Lett., 302, 95–106, 2011.
Mangini, A., Spötl, C., and Verdes, P.: Reconstruction of temperature in the Central Alps during the past 2000 yr from a $d^{18}O$ stalagmite record, Earth Planet. Sci. Lett., 235, 741–751, 2005.
Mattey, D., Fairchild, I. J., Atkinson, T. C., Latin, J.-P., Ainsworth, M., and Durell, R.: Seasonal microclimate control of calcite fabrics, stable isotopes and trace elements in modern speleothem from St Michaels Cave, Gibraltar, in: Tufas and Speleothems: unravelling the Microbial and Physical Controls, edited by: Pedley, H. M. and Rogerson, M., Geological Society, London, Special Publications, 323–344, 2010.
McDermott, F.: Palaeo-climate reconstruction from stable isotope variations in speleothems: a review, Quaternary Sci. Rev., 23, 901–918, 2004.
Mickler, P. J., Banner, J. L., Stern, L., Asmerom, Y., Edwards, R. L., and Ito, E.: Stable isotope variations in modern tropical speleothems: evaluating equilibrium vs. kinetic isotope effects, Geochim. Cosmochim. Ac., 68, 4381–4393, 2004.
Mickler, P. J., Stern, L. A., and Banner, J. L.: Large kinetic isotope effects in modern speleothems, Geol. Soc. Am. Bull., 118, 65–81, 2006.
Miorandi, R., Borsato, A., Frisia, S., Fairchild, I. J., and Richter, D. K.: Epikarst hydrology and implications for stalagmite capture of climate changes at Grotta di Ernesto (NE Italy): results from long-term monitoring, Hydrol. Process., 24, 3101–3114, 2010.
Mühlinghaus, C., Scholz, D., and Mangini, A.: Modelling fractionation of stable isotopes in stalagmites, Geochim. Cosmochim. Ac., 73, 7275–7289, 2009.

CPD
8, 3613–3655, 2012

Rozanski, K., Araguasaraguas, L., and Gonfiantini, R.: Relation between long-term trends of O-18 isotope composition of precipitation and climate, Science, 258, 981–985, 1992.
Scholz, D., Frisia, S., Borsato, A., Spötl, C., Fohlmeister, J., Mudelsee, M., Miorandi, R., and Mangini, A.: Holocene climate variability in North-Eastern Italy: potential influence of the NAO and solar activity recorded by speleothem data, Clim. Past Discuss., 8, 909–952, doi:10.5194/cpd-8-909-2012, 2012.
Smith, C. L., Fairchild, I. J., Spötl, C., Frisia, S., Borsato, A., Moreton, S. G., and Wynn, P. M.: Chronology building using objective identification of annual signals in trace element profiles of stalagmites, Quaternary Geochronol., 4, 11–21, 2009.
Spötl, C. and Vennemann, T. W.: Continuous-flow isotope ratio mass spectrometric analysis of carbonate minerals, Rapid Commun. Mass Sp., 17, 1004–1006, 2003.
Spötl, C., Fairchild, I. J., and Tooth, A. F.: Cave air control on dripwater geochemistry, Obir Caves (Austria): implications for speleothem deposition in dynamically ventilated caves, Geochim. Cosmochim. Ac., 69, 2451–2468, 2005.
Thornthwaite, C. W.: An approach toward a rational classification of climate, Geogr. Rev., 38, 55–94, 1948.
Tremaine, D. M., Froelich, P. N., and Wang, Y.: Speleothem calcite farmed in situ: modern calibration of δ^{18}O and δ^{13}C paleoclimate proxies in a continuously-monitored natural cave system, Geochim. Cosmochim. Ac., 75, 4929–4950, 2011.
Wackerbarth, A., Langebroek, P. M., Werner, M., Lohmann, G., Riechelmann, S., and Mangini, A.: Simulated oxygen isotopes in cave drip water and speleothem calcite in European caves, Clim. Past Discuss., 8, 2777–2817, doi:10.5194/cpd-8-2777-2012, 2012.
Wang, Y. J., Cheng, H., Edwards, R. L., An, Z. S., Wu, J. Y., Shen, C. C., and Dorale, J. A.: A high-resolution absolute-dated Late Pleistocene monsoon record from Hulu Cave, China, Science, 294, 2345–2348, 2001.
Wang, Y. J., Cheng, H., Edwards, R. L., Kong, X. G., Shao, X. H., Chen, S. T., Wu, J. Y., Jiang, X. Y., Wang, X. F., and An, Z. S.: Millennial- and orbital-scale changes in the East Asian monsoon over the past 224 000 year, Nature, 451, 1090–1093, 2008.

CPD
8, 3613–3655, 2012

Table 1. Location and characteristics of caves.

Cave		Altitude (m a.s.l.)	Infiltration Elevation (m a.s.l.)	Aspect	Host Rock[a]	Soil thickness (cm)	Vegetation Type
Bus del Diaol	DL	225	355	W	CG	80	Holm oak forest
Grotta della Bigonda	BG	360	800–1900	N	DP	100	Mixed broadleaf/ conifer forest
Grotta della Fosca	FS	620	650–1300	W	DP	80	Mixed beech/ conifer forest
Grotta Moline	MO	680	1000–2500	SE	CG	80	Conifer forest/ herbs
Grotta Cogola di Giazzera	GZ	1025	1050	SW	CG + dol	40	Mixed beech/ conifer forest
Grotta di Ernesto	ER	1165	1200	NE	CG + dol	100	Mixed beech/ conifer forest
Abisso Spiller	SP	1700	1700	plateau	CG	30	Conifer forest/ Pastures
Grotta Cesere Battisti	CB	1880	1930	NE	CG	20	Dwarf pine, herbs and shrubs

[a] CG: Calcari Grigi limestone, DP: Dolomia Principale dolomite, dol: unspecified dolomite.

CPD
8, 3613–3655, 2012

Table 2. Monitoring and isotopic data from the studied caves.

	Date	$\delta^{13}C_C$ (‰$_{VPDB}$)	$\delta^{18}O_C$ (‰$_{VPDB}$)	$\delta^{18}O_d$ (‰$_{VSMOW}$)	δD_d (‰$_{VSMOW}$)	Drip rate (ml min^{-1})	Cave air pCO_2 (ppm)	Water Temp. (°C)	Frac. Amount (‰)[a]	Stalagmite/ calcite precipitate morphology
ADIGE VALLEY										
Bus del Diaol 225 m a.s.l.										
DL1	19/8/11	−8.55	−7.19	−9.13	−62.8	0.6	2148	11.8	1.53	Top of stalagmite
DL2	19/8/11	−8.28	−6.37	−9.06	−62.1	0.2	6035	11.6	2.24	Calcite precipitate on bulbus stalagmite
DL3[b]	19/8/11	−11.26	−7.27	−9.19	−62.3	17.1	6035	10.9	1.31	Calcite forming micro-gour pool surface
DL4	19/8/11	−9.15	−7.19	−8.86	−60.1	0.3	6035	12.1	1.32	Short flat-topped stalagmite
Grotta Moline 680 m a.s.l.										
MO1	2/2/11	−8.84	−7.72	−9.11	−64.4	0.5	1450	10.1	0.60	Calcite precipitate on sloping wall
MO2	2/2/11	−9.21	−8.16	−9.38	−66.4	0.3	1450	10.6	0.54	Small protruding precipitate on sloping wall
MO3	2/2/11	−9.63	−8.15	−9.48	−67.0	1.5	1450	10.0	0.52	Calcite precipitate on flat part of wall
MO4[b]	2/2/11	−9.57	−8.24	−9.47	−66.3	0.3	1450	10.4	0.51	Calcite precipitate covering wall
MO5	2/2/11	−9.08	−7.99	−9.65	−65.7	3.0	1450	9.9	0.83	Small globular calcite precipitate
MO6	2/2/11	−9.01	−8.10	n.a.	n.a.	no drip	1450	10.2	n.a.	Small globular calcite precipitate
MO7	2/2/11	−9.18	−8.05	n.a.	n.a.	no drip	1450	10.2	n.a.	Small, single bulbus calcite precipitate
Grotta Cogola di Giazzera 1025 m a.s.l.										
GZ1	18/9/10	−8.30	−7.69	−10.20	−70.5	0.092	1170	8.57	1.38	Top of conical stalagmite
GZ2	18/9/10	−7.70	−8.69	−10.44	−73.3	0.021	1170	8.57	0.62	Top of candlestick stalagmite
GZ3	18/9/10	−7.64	−8.39	−10.18	−70.2	0.005	1170	8.57	0.66	Top of candlestick stalagmite
GZ6[b]	18/9/10	−9.09	−8.83	−10.44	−73.4	0.079	1170	8.57	0.48	Top of candlestick stalagmite
Grotta Cesere Battisti 1880 m a.s.l.										
CB1	30/9/10	−1.00	−7.66	−10.64	−72.3	n.a.	577	3.4	0.66	Wall covering drapery, cumulative drips
CB2	30/9/10	−1.50	−7.36	−11.68	−79.2	0.154	577	3.4	2.01	Curtain stalactite feeding cone stalagmite
CB3	30/9/10	−0.46	−7.07	−11.61	−77.4	0.088	577	3.4	2.23	Ceiling precipitate feeding cone stalagmite
CB4	30/9/10	−2.86	−7.45	−11.80	−79.0	0.214	577	3.4	2.04	Patch on flank of larger cone stalagmite
CB5	30/9/10	−2.11	−7.39	−11.22	−76.7	0.638	577	3.4	1.52	Calcite patch on flowstone floor
CB6[b]	30/9/10	−5.86	−7.43	n.a.	n.a.	no drip	577	3.4	n.a.	Precipitate flanking small dome stalagmite

CPD
8, 3613–3655, 2012

Table 2. Continued.

	Date	$\delta^{13}C_C$ (‰$_{VPDB}$)	$\delta^{18}O_C$ (‰$_{VPDB}$)	$\delta^{18}O_d$ (‰$_{VSMOW}$)	δD_d (‰$_{VSMOW}$)	Drip rate (ml min^{-1})	Cave air pCO_2 (ppm)	Water Temp. (°C)	Frac. Amount (‰)[a]	Stalagmite/ calcite precipitate morphology
VALSUGANA VALLEY										
Grotta della Bigonda 360 m a.s.l.										
BG1	9/8/10	n.a.	n.a.	−8.64	−55.6	98	n.a.	n.a.	n.a.	
BG1	6/9/10	−7.62	−7.11	−8.51	−57.1	107	600	8.1	0.29	Rim of dome stalagmite with large drip pit
BG1	19/2/12	n.a.	n.a.	−9.02	−58.5	56	450	n.a.	n.a.	
BG2	9/8/10	n.a.	n.a.	−8.71	−61.5	5.8	n.a.	n.a.	n.a.	
BG2	6/9/10	−7.17	−6.84	−8.62	−60.5	2.9	520	8.1	0.63	Top of stalagmite
BG2	19/2/12	n.a.	n.a.	−8.83	−57.9	2.0	400	n.a.	n.a.	
BG2	9/8/10	n.a.	n.a.	−8.71	−59.0	2.6	n.a.	n.a.	n.a.	
BG2	6/9/10	−6.49	−7.03	−8.92	−56.6	2.7	520	8.1	0.45	Thin, precipitate flanking larger stalagmite
BG3	19/2/12	−7.31	−6.98	−8.96	−58.4	3.0	400	7.5	0.61	Small dome stalagmite
BG4	6/9/10	−8.12	−6.85	−8.75	−58.6	9.4	580	8.1	0.67	Top of stalagmite
BG4	19/2/12	n.a.	n.a.	−8.41	−54.9	3.1	440	n.a.	n.a.	
BG5	19/2/12	−7.47	−6.69	−8.48	−56.6	1.4	440	6.9	0.28	Top of stalagmite
BG6	6/9/10	−8.25	−7.50	−9.00	−59.7	7.8	580	8.1	0.26	Thin, precipitate flanking larger stalagmite
BG6	19/2/12	n.a.	n.a.	−9.16	−59.9	5.8	440	n.a.	n.a.	
BG7[b]	19/2/12	−8.80	−7.05	−9.19	−59.5	0.8	440	6.2	0.47	Small stalagmite as part of large column
Grotta della Fosca 620 m a.s.l.										
FS1[b]	10/9/10	−10.18	−7.12	−8.91	−61.7	1.20	1540	8.0	0.53	Small bulbus stalagmite/flowstone on rock
FS2	10/9/10	−9.51	−6.90	−8.97	−61.9	2.00	1540	7.8	0.77	Thin, "brain-like" calcite flowstone on rock
FS3	10/9/10	−8.64	−7.31	−9.51	−63.9	0.17	1540	8.3	1.01	Small bulbus stalagmite
FS4	10/9/10	−5.70	−6.54	−9.47	−63.3	0.06	1590	8.6	1.81	Thin precipitate flanking larger stalagmite
FS5	10/9/10	−8.57	−7.46	−9.50	−62.8	0.21	1590	8.3	0.85	Small precipitate on flat broken stalagmite
FS6	10/9/10	−6.58	−6.09	−9.10	−58.5	0.05	1590	8.6	1.88	Flat topped small stalagmite
Grotta di Ernesto 1165 m a.s.l.										
ER1	7/9/10	−8.15	−6.98	−9.54	−63.0	3.3	1410	7.15	1.11	"Brain-like" calcite flowstone
ER2	7/9/10	−9.27	−7.03	−9.44	−60.5	2.4	1400	7.15	0.96	Top of stalagmite
ER3	7/9/10	−8.07	−7.16	−9.43	−60.4	0.1	1400	7.15	0.82	Top of large round stalagmite
ER4[b]	7/9/10	−9.32	−7.53	−9.51	−63.7	0.17	1430	7.15	0.52	Top of small dome stalagmite
ER5	7/9/10	−8.22	−6.90	−9.47	−59.1	0.078	1350	7.15	1.11	Top of stalagmite
ER6	7/9/10	−7.79	−6.52	−9.47	−62.1	0.011	1350	7.15	1.50	Top of small stalagmite
ER7	7/9/10	−7.13	−6.77	−9.45	−63.4	0.022	1350	7.15	1.23	Top of small rounded stalagmite
ER8	7/9/10	−7.76	−6.42	−9.74	−62.2	0.018	1350	7.15	1.87	Top of small rounded stalagmite

CPD
8, 3613–3655, 2012

Table 2. Continued.

	Date	$\delta^{13}C_C$ (‰$_{VPDB}$)	$\delta^{18}O_C$ (‰$_{VPDB}$)	$\delta^{18}O_d$ (‰$_{VSMOW}$)	δD_d (‰$_{VSMOW}$)	Drip rate (ml min^{-1})	Cave air pCO_2 (ppm)	Water Temp. (°C)	Frac. Amount (‰)[a]	Stalagmite/ calcite precipitate morphology
Abisso Spiller 1700 m a.s.l.										
SP1	12/9/10	−6.83	−7.17	−9.77	−66.8	3.4	827	4.3	0.49	Small precipitation on broken stalagmite
SP2	12/9/10	−3.05	−6.71	−9.70	−65.2	0.46	827	3.7	0.74	Top of conical stalagmite
SP3	12/9/10	−1.82	−6.57	−9.87	−66.3	0.15	827	3.7	1.05	Top of small dome stalagmite
SP4	12/9/10	−4.41	−6.86	−9.98	−65.9	0.35	827	3.6	0.85	Precipitate in large drip pit
SP5	12/9/10	−4.12	−6.95	−9.93	−66.8	4.5	827	3.4	0.66	Top of conical stalagmite
SP6[b]	12/9/10	−7.29	−7.42	−9.97	−65.7	23.0	827	3.7	0.31	Precipitate on bulbus flowstone wall

[a] Fractionation Amount calculated as the difference between the measured oxygen isotope value of the cave calcite and that calculated based on the cave temperature and the dripwater oxygen isotope composition (Kim and O'Neil, 1997).

[b] Selected "least fractionated" sample from each cave according to Fig. 6.

n.a. not analysed in the case of BG cave where the parameter was measured on another occasion or not applicable where there was no dripwater present or drip rate could not be measured as water was collected from multiple sources.

CPD
8, 3613–3655, 2012

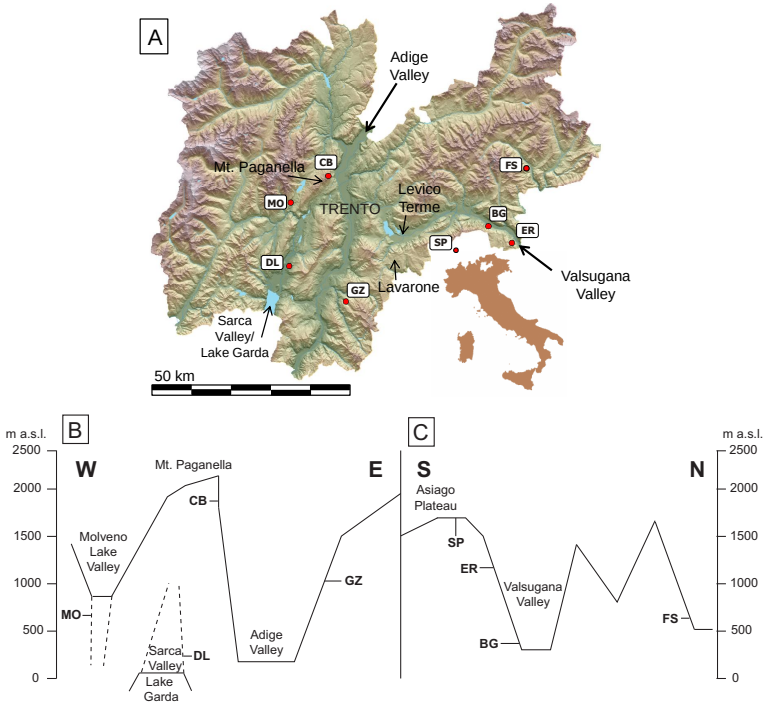

Fig. 1. Location of cave sites in Trentino, N. Italy. **(A)** Map of Trentino with cave sites and main valleys marked on. Note SP Cave is just in the Veneto region. **(B)** Schematic cross-section of topography to show the relative altitudes and locations of the cave sites in and around the Adige Valley. Internal valleys are noted with dashed lines. **(C)** Schematic cross-section of caves of the Valsugana Valley. Altitudes are to scale, horizontal length is schematic.

CPD
8, 3613–3655, 2012

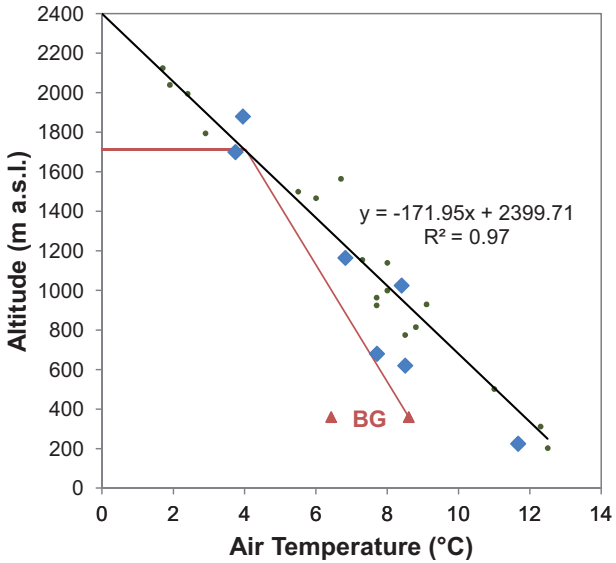

Fig. 2. Air temperature of meteorological stations and cave interiors against altitude. Green dots indicate average air temperature at 2 m over the period 1961–1990 at 19 long-running weather stations in Trentino (http://www.meteotrentino.it). Blue diamonds represent the air temperature from of the stable interior cave air for each of the caves (except BG) at the time of monitoring. Bigonda Cave (BG red triangles; summer and winter range) falls below the expected temperature for the elevation of the cave entrance. The red line from the stable summer temperature uses an adiabatic lapse rate value of 3.4 °C km^{-1} (similar to the value stated for the deep vadose zone of the conceptual model of temperature distribution in a karst aquifer, Luetscher and Jeannin, 2004 and between that of humid air calculated from the regions rainfall as 0.56 °C/100 m and a value of 0.234 °C/100 m for vertical transit of water through a completely saturated aquifer, Luetscher and Jeannin, 2004) to gain an approximate infiltration elevation for BG cave as 1700 m, based on temperature, which is the actual elevation of the karst plateau above the cave.

CPD
8, 3613–3655, 2012

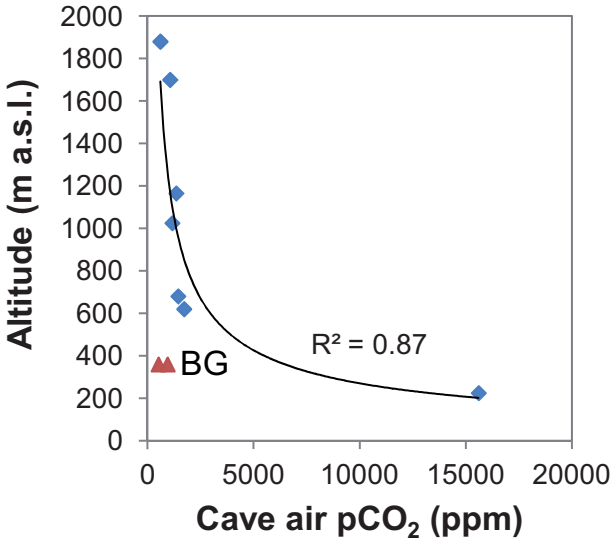

Fig. 3. Cave air carbon dioxide concentration against cave entrance altitude. Blue diamonds represent the stable innermost cave carbon dioxide concentration during the monitoring trip, with the exception of BG cave (red triangles) that are excluded from the trend. The two BG values are from summer and winter monitoring trips.

CPD
8, 3613–3655, 2012

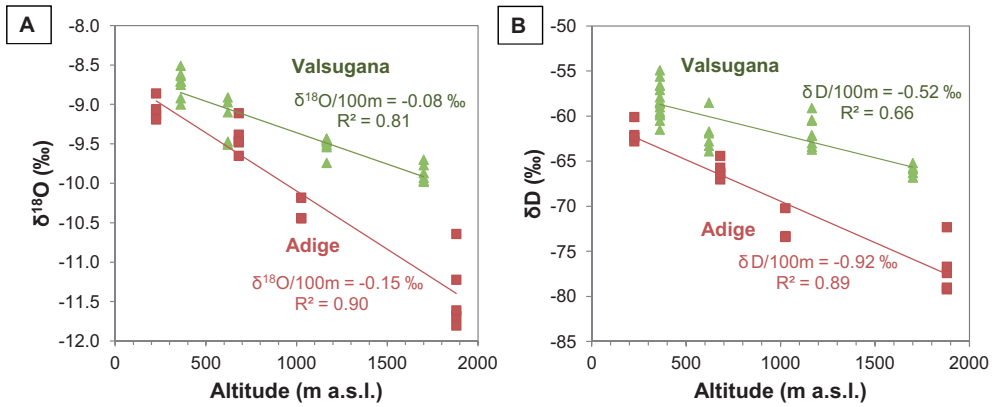

Fig. 4. Oxygen and hydrogen isotopes of the dripwaters in caves from different altitudes. **(A)** The oxygen isotope values deviate depending on which valley (Adige or Valsugana) the caves are situated (see Fig. 1). **(B)** Hydrogen isotopes follow a similar pattern as the oxygen isotopes in the two valleys.

CPD
8, 3613–3655, 2012

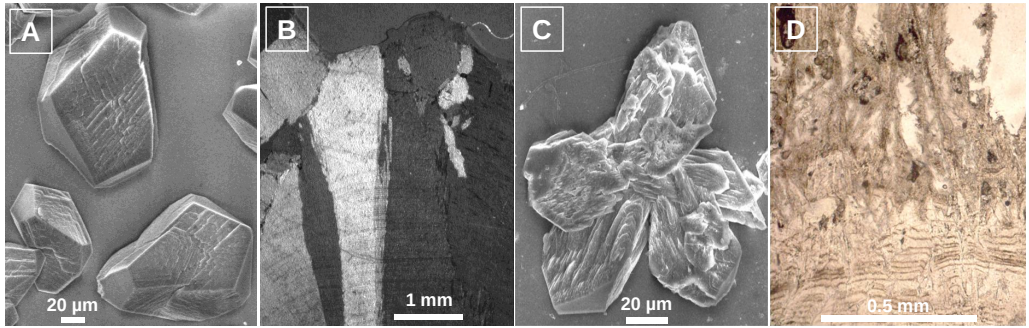

Fig. 5. Petrography of cave calcite precipitates and corresponding stalagmite fabrics. **(A)** Calcite precipitate on glass slide collected in DL cave between June and September 2003. SEM image shows large crystals with a predominance of flat faces. **(B)** Optical microscope image (crossed polars) of the top of stalagmite SP1 from SP cave that was active at the time of sampling (2003). Image shows columnar fabric of both compact and microcrystalline subtypes developing from crystals similar to those shown in **(A)**. **(C)** Calcite precipitate on glass slide collected over a 1-yr period in ER cave from December 2003. The SEM image shows many macrosteps and macrokinks on the irregular faces. **(D)** Optical microscope image of typical fabrics of stalagmite ER77. (Bottom) Annually laminated microcrystalline subtype of columnar fabric grading into highly porous dendritic fabric (top) arising from irregular crystals with lateral overgrowths as shown in **(C)**.

CPD
8, 3613–3655, 2012

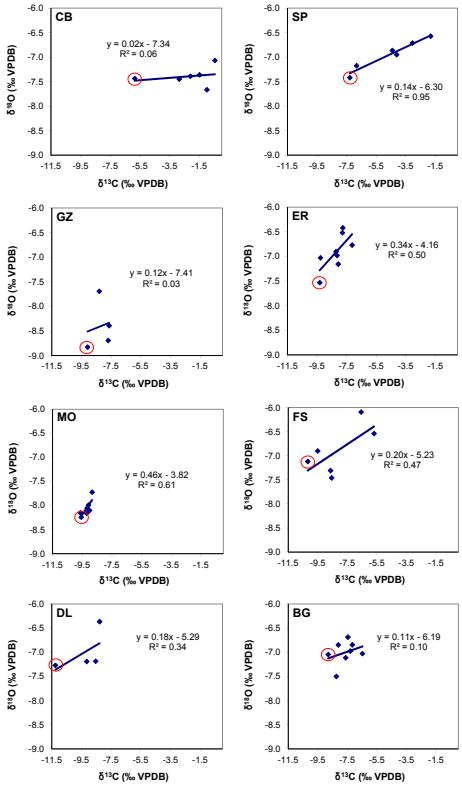

Fig. 6. Cross-plots of $\delta^{13}C$ and $\delta^{18}O$ for recent calcite precipitates from the studied cave sites. The plots show the extent of in-cave variability between samples caused by physical factors (e.g. drip rate, drip height) and subsequent kinetic fractionation. Red circles indicate the least fractionated sample from each cave, chosen to demonstrate principles in the discussion part of this paper (Sect. 5).

CPD
8, 3613–3655, 2012

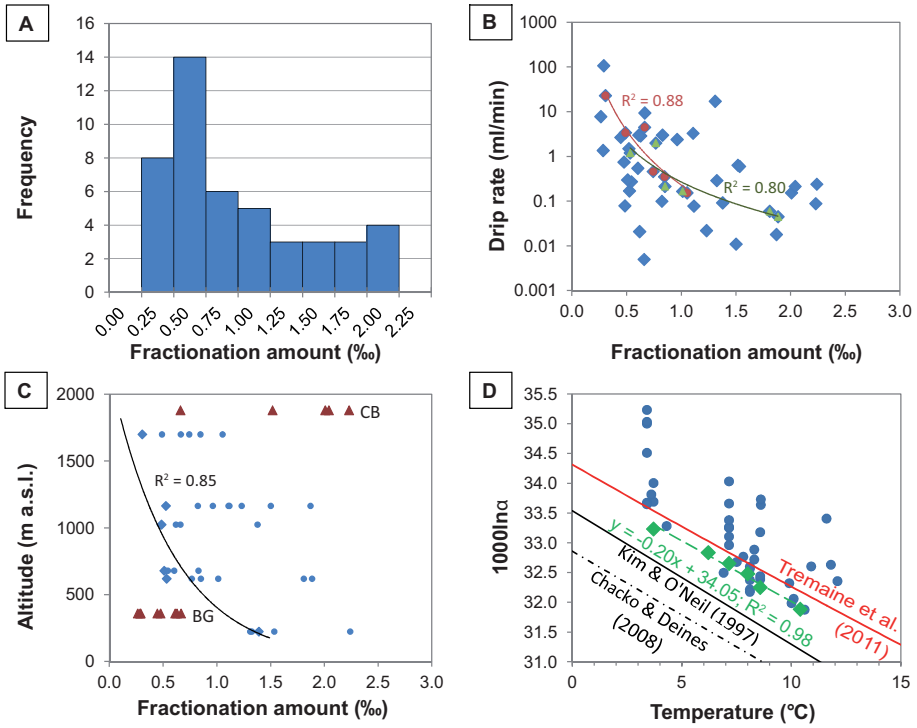

Fig. 7. (Caption on next page.)

CPD
8, 3613–3655, 2012

Fig. 7. Distribution of fractionation amount and its correlation with drip rate, altitude and temperature. Fractionation amount calculated as the difference between the measured oxygen isotope composition of speleothem calcite and theoretical values based on the equations of Kim and O'Neil (1997) using the measured dripwater $\delta^{18}O$ and the dripwater temperature. **(A)** Histogram showing the frequency of fractionation amounts from all caves monitored in this study. **(B)** Fractionation amount plotted against the drip rate of each corresponding drip point. Trend lines show examples for individual cave sites of SP cave (red circles) and FS cave (green triangles). **(C)** Fractionation amount plotted against the altitude of the cave entrance. Measurements from all cave sites plotted as blue circles, with the exception of those from BG and CB caves plotted as red triangles and excluded from the trend. The trend line is formed using only the favoured, "least-fractionated" (see Fig. 6) examples from each cave site (blue diamonds). **(D)** $1000 \ln \alpha$ for all cave samples (blue dots) estimated as $\delta^{18}O_{calcite}$ minus $\delta^{18}O_{drip}$ (‰$_{VSMOW}$). Green diamonds indicate the values of the "least fractionated" examples, with the exception of DL cave where all samples measured in this study exhibited over 1 ‰ fractionation amount and CB cave where the least fractionated example does not have a corresponding dripwater. The red line indicates an empirical palaeotemperature relationship for water-calcite oxygen isotope fractionation of speleothems from the literature (Tremaine et al., 2011). The black solid and the dot-dashed lines represent the $1000 \ln \alpha_{(Calcite\text{-}H_2O)}$ found experimentally by Kim and O'Neil (1997) and theoretically from Chacko and Deines (2008), respectively.

CPD
8, 3613–3655, 2012

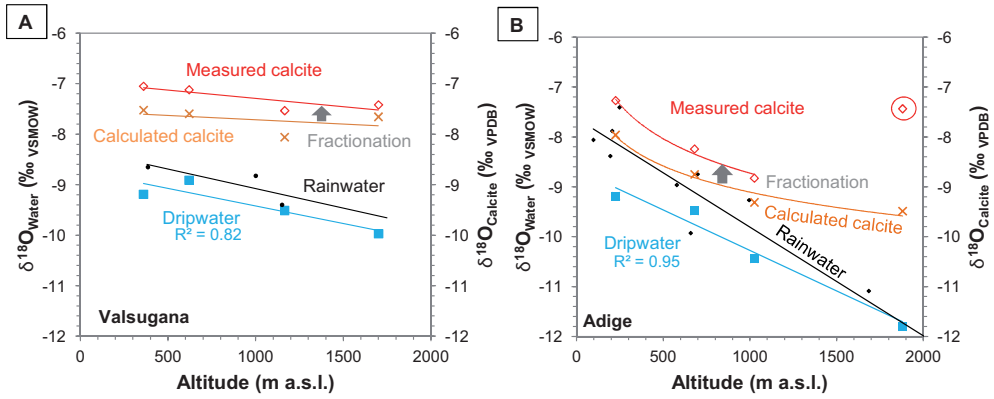

Fig. 8. Oxygen isotope values of the **(A)** Valsugana and **(B)** Adige Valleys plotted against altitude. Annual weighted-average rainwater values are shown in black dots (Bertò et al., 2005), cave dripwaters (solid blue squares) and corresponding calculated (Kim and O'Neil, 1997) and measured calcite precipitates (orange crosses and red open diamonds, respectively). The calcite points plotted represent only one sample from each cave that we consider to be the least fractionated (see Fig. 6). This plot therefore serves to explain the (relatively) un-fractionated processes occurring in the cave and not to show an exhaustive range of possible $\delta^{18}O$ values. DL calculated calcite has been computed based on long-term monitoring of the cave dripwater, rather than a one-off sample, using the $\delta^{18}O$ value of -8.31 ± 0.23 ‰$_{VSMOW}$. One outlier has been identified in the measured calcite data of B, that of CB cave (1880 m). Note waters plotted on VSMOW scale and calcite plotted against VPDB, and therefore values are not directly comparable.

CPD
8, 3613–3655, 2012

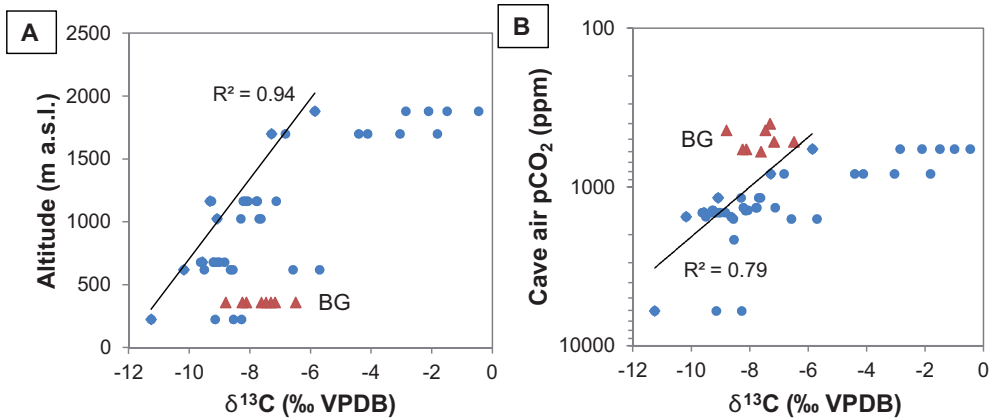

Fig. 9. Carbon isotope values against **(A)** the altitude of the cave entrance, and **(B)** the cave air pCO_2 measured during the monitoring trip at the chosen drip site. Note the inverse logarithmic scale, where values at the top of the graph generally correspond to high altitude. BG cave data, marked as red triangles, does not fit the trend with the other cave sites. The trend lines have been drawn using just the "least fractionated" calcite precipitates from each cave site (see Fig. 6), excluding BG, but represent the overall pattern shown by the complete dataset.

CPD
8, 3613–3655, 2012